Crack-Healing Behavior of Epoxy–Amine Thermosets

M. Aflal M. Rahmathullah, Giuseppe R. Palmese

Department of Chemical and Biological Engineering, Drexel University, Philadelphia PA 19104

Received 18 August 2008; accepted 23 November 2008
DOI 10.1002/app.30152
Published online 27 April 2009 in Wiley InterScience (www.interscience.wiley.com).

ABSTRACT: This work offers detailed experimental evidence for crack healing in fully formed epoxy–amine polymer networks. Compact tension specimens of diglycidyl ether of bisphenol A (EPON-828) and 4,4′-methylene biscyclohexanamine were synthesized at stoichiometry and with an excess or paucity of an amine curing agent. Healing efficiencies were measured on the basis of the regain in the fracture load after a healing protocol was applied. For all systems investigated, the average healing efficiency for first fracture was greater than 50% when healing was conducted at 185°C for 1 h. The crack-healing behavior was highly repeatable at all stoichiometries, and healing was found to occur for repeated fracture–heal cycles of the same specimen. On the basis of results from size exclusion chromatography for the extractable phase, infrared spectroscopy, and scanning electron microscopy, it is postulated that healing is primarily due to mechanical interlocking of the nodular topology of a fractured crack interface that occurs in the rubbery state and is set in place by vitrification upon cooling. A ½ power dependence of the healing efficiency on the healing time was observed, and this suggests that the interlocking of topographical features is governed by diffusive processes. For networks cured with a large excess of epoxide groups, the recovered fracture load was higher than that of virgin specimens. In this case, polyetherification or homopolymerization of previously unreacted epoxy groups increased the healing efficiency significantly, and this suggests that low degrees of covalent bonding can significantly enhance healing behavior in these systems.
 J Appl Polym Sci 113: 2191–2201, 2009

Key words: fracture; networks; thermosets

INTRODUCTION

Highly crosslinked thermosetting polymers are used extensively in adhesives, structural composites, and protective coatings. They exhibit excellent thermal and mechanical performance as well as solvent resistance.[1] Epoxy thermosets are generally brittle and are often used in conjunction with toughening agents such as rubber modifiers[2] or thermoplastic additives[3] that improve fracture toughness but reduce properties such as the modulus and glass-transition temperature (T_g). The inherent brittleness of epoxies leads to incipient microcrack formation due to thermal or mechanical cycling. These microcracks can coalesce over operational lifetimes to eventually cause unexpected macroscopic fracture. One approach used to mitigate the effects of microcrack growth is the design of self-healing material systems that can reverse damage and recover load-bearing capacity.

A number of self-healing techniques have been explored for brittle materials over the last 2 decades. In early work by Dry,[4] hollow fibers filled with reactive liquids were embedded in concrete; they ruptured on failure and filled cracks to cause strength recovery. More recently, White et al.[5] developed polymer composites that heal autonomously. In these systems, microcapsules filled with monomers are dispersed within a catalyst-containing matrix. Upon failure, the microcapsules rupture, releasing monomers that fill the crack site and react when exposed to the catalyst particles. Similar work by Bond et al.[6] has shown the healing behavior of fiber-reinforced epoxy composites into which resin-filled hollow glass fibers have been incorporated. Such techniques have demonstrated the design of systems that can heal autonomously at least once. However, the need to develop materials that can heal multiple times without severe loss in strength is evident because once the filled inclusions are ruptured, the healing agent is depleted. Remendable systems based on reversible covalent Diels–Alder linkages, as investigated by Chen and coworkers,[7,8] and healing via the incorporation of linear polymer chains, as reported by Hayes et al.,[9] show promise as continuously rehealable material systems. However, despite the growing number of studies dedicated to finding healing additives for common thermoset systems

Correspondence to: G. R. Palmese (palmese@coe.drexel.edu).
Contract grant sponsor: Army Materials Center of Excellence; contract grant number: W911NF-O6-2-0013.

TABLE I
Healing Efficiencies from Other Researchers Versus the Healing Efficiency of This Study's Epoxy–Amine Thermoset

Method	Healing efficiency (%)
Autonomic healing[5]	80–90
Retro Diels–Alder[7]	60–80
Polymer blends[9]	40
Anhydride-cured epoxy[10]	100
Vinyl ester[19]	1.7
This study's system	>50

such as amine-cured epoxies, there has been very limited work reporting the inherent healing capacity of unmodified thermosets. This is not surprising because the crosslinked nature of thermosets is expected to curtail healing mechanisms observed for thermoplastics. Yet, surprising results briefly mentioned in the literature suggest that healing is possible in crosslinked epoxy systems.[10,11] Our own preliminary results have shown that certain unmodified amine-cured epoxies show healing efficiencies comparable to those observed in currently used healable thermosets, as summarized in Table I. Therefore, investigating the healing behavior of neat thermosets serves two main purposes: first, to establish a baseline behavior to which developments can be compared, and second, to provide insights into the mechanisms of thermoset healing that could lead to novel strategies for incorporating healing capacity into multifunctional composite structures. The work reported herein represents the first detailed crack-healing study of unmodified epoxy–amine networks. The investigated system is a diglycidyl ether of bisphenol A (DGEBA) cured with a cycloaliphatic diamine. DGEBA forms the basis for many commercial systems,[12] systems investigated by our group,[13,14] and also those of others.[15] The crack-healing behavior of epoxy–amine thermosets was evaluated with a modified compact tension test protocol. The influence of healing conditions such as the time and pressure on strength recovery was evaluated for single healing experiments as well as cyclic healing experiments. Additionally, the influence of epoxy–amine stoichiometry on healing behavior was assessed. The obtained data provide valuable clues regarding the mechanism of healing in these systems.

EXPERIMENTAL

Materials

DGEBA (EPON-828, n = 0.13; Miller-Stephenson), tetrafunctional amine, 4,4′-methylene biscyclohexanamine (PACM; Air Products), and tetrahydrofuran (THF; 99.9%; Sigma–Aldrich) were used as obtained. The chemical structures of the monomers used are shown in Figure 1.

Sample preparation

The composition of the epoxy–amine samples used in this study is given in Table II. Samples at stoichiometry were synthesized with an epoxy–amine weight ratio of 100 parts of epoxy to 28 parts of amine. This corresponds to a stoichiometric ratio of epoxide groups to reactive amine hydrogen groups that is defined as $r = 1.0$. All samples synthesized off stoichiometry were identified on the basis of this r value so that samples made with excess epoxy had $r > 1.0$ and samples with excess amine had $r < 1.0$. All values of r were accurate within ± 0.02. The reaction mixtures were homogenized and degassed at room temperature with a planetary motion mixer (Model AR250, Thinky Corporation, USA).

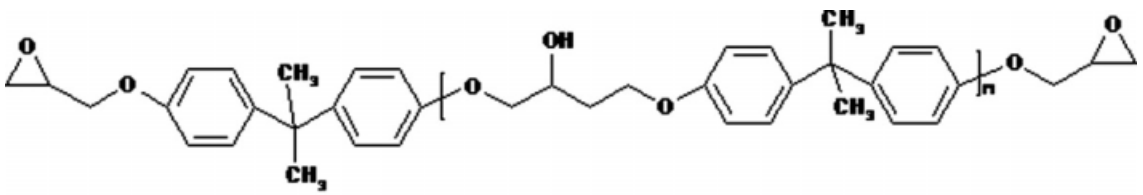

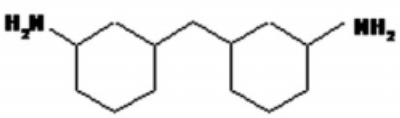

Figure 1 Chemical structures of monomers used for the synthesis of the epoxy–amine thermosets.

TABLE II
Weight and Molar Ratios of EPON-828 and PACM used for the Synthesis of Epoxy–Amine Thermosets

EPON-828	PACM	EPON-828/PACM ratio by weight	EPON-828/PACM molar ratio
100	20	5.00	1.40
100	23	4.35	1.20
100	26	3.85	1.07
100	28	3.58	1.00
100	32	3.13	0.88
100	34	2.94	0.82

Subsequently, a cure schedule of 80°C for 2 h and 165°C for 2 h was used to ensure the complete conversion of epoxy and amine groups at $r = 1.0$.[16] For mechanical testing, samples were machined to the required dimensions according to ASTM D 5045-99. A single hole was drilled at a distance of 3.5 mm from the notched end following the method of Chen et al.[8] to arrest the propagating crack.

Test protocol and healing efficiencies

Figure 2 shows a schematic of the compact tension test specimen used to evaluate the healing efficiency. A starter crack was created at the base of the notch by gentle tapping with a sharp razor blade. The test specimens were loaded in tension between clevis grips with dowel pins at a crosshead speed of 0.1 mm/min, and the experiment was stopped as soon as the crack was arrested by the hole. With the crack arrested in this fashion, the fractured faces of the specimen could be accurately realigned. For this arrangement, the crack length remained constant at 3.5 ± 0.1 mm. The fractured specimens were healed by either a high-pressure method (HP) or a low-pressure (LP) method. In the former, the specimens were kept between 8 and 13 MPa with a heated press and allowed to heal at a set temperature and time. In the latter, a pressure of 0.13 MPa was applied in a pre-equilibrated convection oven. All healing studies were done in air, and all specimens showed a visual disappearance of the crack interface before testing. For all tests, four to six individual specimens were used to compute fracture loads and healing efficiencies.

The healing efficiencies were computed with the following equation:

$$\varepsilon_n = \frac{P_n}{P_0} \times 100 \quad (1)$$

where ε_n is the healing efficiency at the nth cycle, P_n is the maximum load at fracture at the nth cycle, and P_0 is the load at fracture of the original specimen. For cyclic healing tests, the healing efficiency based on the previous load (ε'_n) is defined as follows:

$$\varepsilon'_n = \frac{P_{n+1}}{P_n} \times 100 \quad (2)$$

For example, Table III provides values of healing efficiencies measured for specimens with the HP or LP method at different stoichiometries at a healing

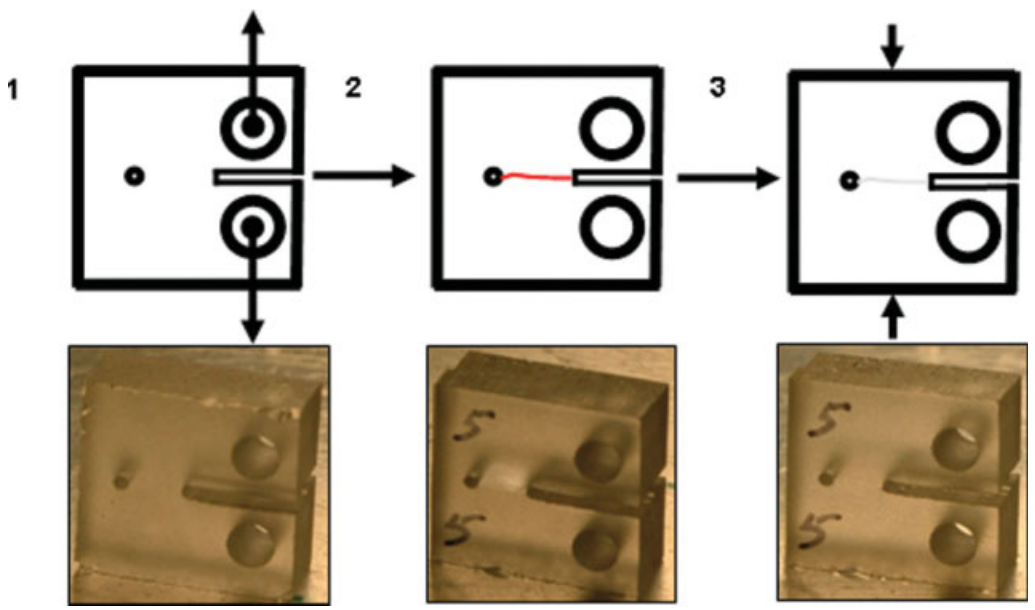

Figure 2 Schematic and photographs showing the test procedure used: (1) a compact tension specimen loaded under tension at 0.1 mm/min, (2) a compact tension specimen with an arrested crack, and (3) a specimen healed with either the HP method or the LP method. [Color figure can be viewed in the online issue, which is available at www.interscience.wiley.com.]

TABLE III
Fracture Loads and Healing Efficiencies Before and After the First Heal Measured with the HP and LP Methods at Different *r* Values

	ε_1 (%)	
r	HP method	LP method
0.82	53	47
1.00	60	39
1.07	42	32

temperature (T_{heal}) of 185°C and a healing time (t_{heal}) of 1 h. It is apparent from the data at $r = 1.0$, $r = 0.88$, and $r = 1.07$ that the HP method resulted in a higher healing efficiency at all stoichiometries. On the basis of these results, all further testing reported in this work was carried out with the HP method.

Size exclusion chromatography (SEC)

SEC was used to determine the presence of leachable extracts in cured epoxy–amine thermosets at different stoichiometries. A Waters 515 (Waters Corporation, Milford, MA) gel permeation chromatograph pump was used with two 30-cm-long, 7.5-mm-diameter, 5-μm styrene/divinyl benzene columns in series (PL gel, Polymer Laboratories, Amherst MA; 50-Å pore size and mixed C for the first and second columns, respectively). The columns were equilibrated and run at 30°C with THF as the elution solvent at a flow rate of 1 mL/min. The column effluent was monitored with a Waters 2410 refractive-index detector. Samples were prepared by the immersion of 0.02 g of a cured epoxy–amine specimen per gram of THF and equilibrated at 60°C. The extract was filtered through a Nalgene 0.45-μm syringe filter before injection into the column.

Scanning electron microscopy (SEM)

Morphological characterization was carried out with an FEI model XL30 (FEI Company, Hillsboro, OR) field-emission gun environmental scanning electron microscope at an accelerating voltage of 10 kV and with a spot size of 3. All samples were sputter-coated with platinum before analysis.

Fourier transform infrared (FTIR)

FTIR analysis was performed with a Nicolet Nexus 670 spectrometer (Thermo Electron Corporation, Waltham, MA) between 4000 and 8000 cm^{-1} with a DTGS KBr detector at an aperture setting of 100. The resolution was set at 8 cm^{-1}, and 32 scans were taken per spectrum. Epoxy group concentrations were monitored at a wavelength of 4528 cm^{-1}, whereas secondary amine N—H stretching overtones were monitored at 6480 cm^{-1}.[14,17,18]

Differential Scanning Calorimetry (DSC)

T_g of the thermosets was obtained with differential scanning calorimetry (DSC; Q2000 TA Instruments, New Castle, DE) and measured from the second heating scan at 10°C/min between 30 and 200°C. Samples ranged in weight from 5 to 12 mg and were placed in sealed aluminum pans.

RESULTS AND DISCUSSION

The results of the healing experiments are presented in two sections. The crack-healing behavior of epoxy–amine thermosets evaluated at stoichiometry ($r = 1$) is discussed first, and this is followed by the healing behavior off stoichiometry ($r \neq 1$).

Healing behavior at $r = 1$

Figure 3 shows a plot of the fracture load and rehealing efficiency for fully cured samples synthesized at $r = 1.0$ and measured over repeated fracture and heal events. The fractured samples were rehealed at every cycle ($t_{heal} = 1$ h and $T_{heal} = 185$°C) with the HP method. The average fracture load of virgin specimens was 68 N. The average fracture load was progressively lower after each heal with an average value of 37 N after the fourth cycle. The regains in fracture load correspond to ε_n values of 68, 60, 50, and 43% for the first, second, third, and fourth cycles, respectively. These values of ε_n are all significantly higher than the 1.7% recovery observed

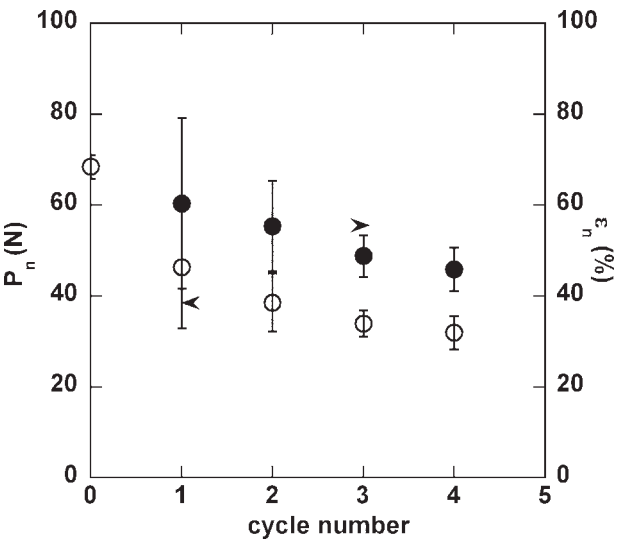

Figure 3 Representative plot for samples with $r = 1.0$ showing repeated regain in (●) the healing efficiency and (○) the fracture load. The samples were healed at $T_{heal} = 185$°C under HP.

for a vinyl ester.[19] The data in Figure 3 also indicate that the fracture load measured upon repeated healing is always less than the previously measured fracture load.

The contributions of surface energy towards healing is thought to be minimal since the surface energy for an epoxy is typically around 50 mJ/m^2,[10,20] whereas the observed fracture energies are closer to 100 J/m^2. One explanation for the observed healing is the possibility of chemical reactions resulting in covalent bonding at the interface. Exposure of epoxy–amine thermosets to elevated temperatures may cause etherification reactions in the presence of epoxide groups. Near-infrared spectra of fully cured specimens with $r = 1.0$ did not show unreacted epoxide or amine groups and indicated full conversion of epoxides and amines. T_g determined from DSC thermograms did not change appreciably with time and remained constant at 162.3 ± 1.4°C after 180 min of heating at 185°C. This further supports the contention of insignificant changes due to reactions occurring in the sample at T_{heal}.

The effect of postcure on healing characteristics was further explored by annealing studies of fractured specimens. Epoxy–amine specimens with $r = 1.0$ were fractured and annealed for 1 h at 185°C, and the crack interface was forced apart to avoid contact between fractured surfaces. Samples were then healed at 185°C under HP for 1 h. The average fracture load of virgin specimens was 80.1 ± 16.5 N, and the average fracture load after healing was 51.7 ± 2.9 N with an average healing efficiency for first fracture (ε_1) of 70.6 ± 11.7%. This healing efficiency was comparable to that of nonannealed specimens, as shown in Figure 3. This result further eliminated the reaction as a major healing mechanism for systems cured at stoichiometry.

Another possible explanation for the observed healing is the interpenetration of a polymeric sol phase from one side of the fracture surface to the other in a manner comparable to the mechanism of healing observed in thermoplastic materials.[21] However, SEC extracts from specimens cured at stoichiometry did not possess a measurable leachable fraction to suggest the presence of a mobile phase within the thermoset. Hence, our results for $r = 1.0$ support the absence of a reactive interface and a mobile phase that could explain the observed healing behavior.

Figure 4 shows a plot of ε_1 in samples after the first fracture/heal event for specimens with $r = 1.0$ versus t_{heal} at 185°C. From a least-squares fit of data at short times ($t_{heal} < 30$ min), the healing efficiency was found to depend on time to the power of $1/2$. The data show that for this case, the healing efficiency does not reach 100% but appears to plateau at approximately 55 min at a lower value. According

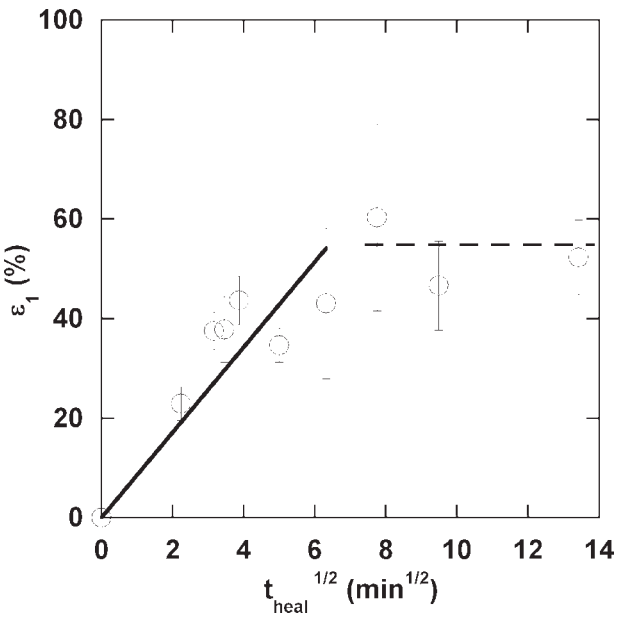

Figure 4 Plot of ε_1 versus $t_{heal}^{1/2}$ for samples with $r = 1.0$

to theories developed for the welding of linear polymers, the fracture energy is dependent on t_{heal} to the power of $1/2$, whereas the stress intensity factor and fracture stress are dependent on t_{heal} to the power of $1/4$.[11] The data from Figure 4 indicate that ε_1 (which is a measure of the fracture load recovery and is proportional to the fracture stress) has a $1/2$ power dependence, suggesting deviations from theories developed for linear polymer systems.[21–23] This might be so because unattached molecules are not available for entanglement in such a highly crosslinked thermoset.

The development of chain entanglements upon healing in polymer thermosets cannot be described by the reptation model developed for linear polymers[23,24] because of the absence of long polymer chains unattached to a polymer network. Healing in epoxy–amine polymer networks might be due to entanglements of fractured and dangling chain ends; this is similar to explanations for the crack healing of polyurethanes[25] or crosslinked polystyrene-*co*-polyacrylonitrile.[22] Compared to the long-range interpenetration found in high-molecular-weight thermoplastic welding, short-range dangling chain end interpenetration would not provide, on its own, high healing efficiencies. However, the adhesive effects of such short chain entanglements could be enhanced by the presence of a topologically irregular and rough fracture surface because the interfacial contact area in such a case would be higher, allowing for a greater volume of interaction through interpenetration.

In trying to elucidate the healing mechanism of crosslinked epoxy–amine thermosets, it is also useful

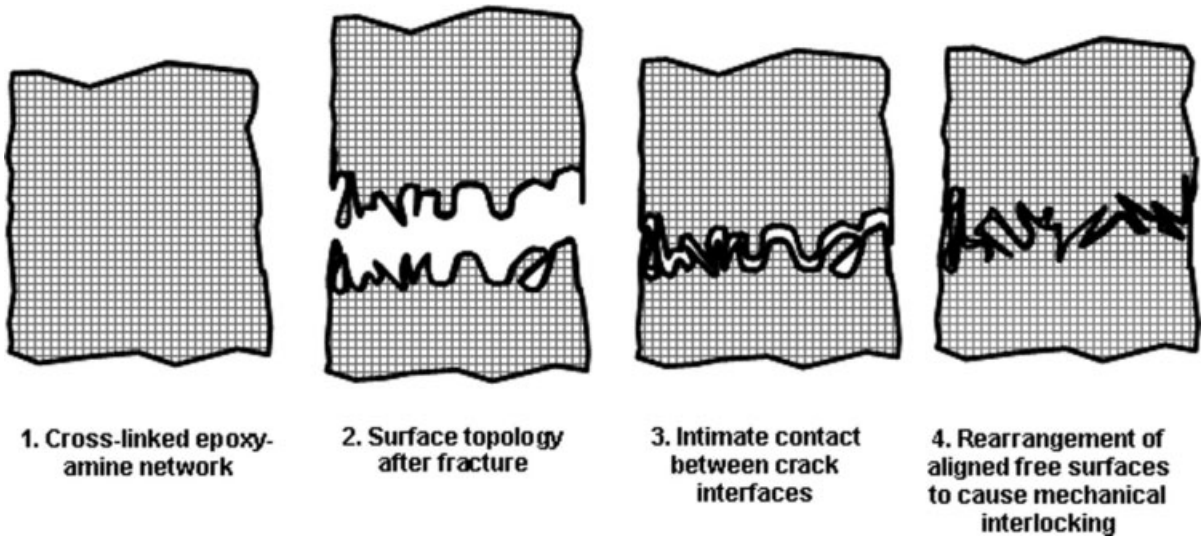

Figure 5 Schematic of a possible phenomenon for healing at a crack interface where adhesive strength may be developed through mechanical interlocking of surface topological features.

to assess the timescales for candidate processes in relation to the observed healing phenomena. A terminal chain in our fully cured system at stoichiometry would essentially consist of a polymer repeat unit ($\sim$ 796 g/mol). The diffusivity of such chain ends at short times is conservatively approximated to be 10^{-10} m^2/s,[26] and this corresponds to a 1-nm diffusion depth being crossed in the order of 10^{-8} s. Because the observed crack-healing process occurs over many minutes as shown in Figure 4, this is not the principal process responsible for strength recovery. A far slower step would be the rearrangement of larger scale surface features.

The surface topography of fractured epoxy thermosets varies, depending on the type of curing agent, cure schedule, and measurement technique.[27–30] The fracture surfaces generally appear to have a nodular topography. From AFM measurements,[27–30] the average height of each nodule (the root mean square distance) appears to vary largely between 5 and 200 nm and may be considered a characteristic length that interacts on either side of a fractured surface. When fractured surfaces come in contact during healing, the peaks and valleys will most likely not match perfectly at the nanoscopic scale, and this will limit contact and bonding. An applied pressure and a temperature above T_g allow rearrangement of the surface topography to maximize contact and interpenetration at the polymer–polymer interfaces. Upon cooling below T_g, permanent mechanical interlocking responsible for strength recovery will occur. A schematic of this postulated mechanism is given in Figure 5, in which the presence of a nodular fracture morphology enhances mechanical adhesion by Velcro-like entanglements. If we use the Einstein diffusion equation[31,32] as an approximation for the rearrangement above T_g of surface features at an average height of 102 nm (presumed to be a mean displacement responsible for interlocking), the nodule diffusivity will be of the order of 10^{-18} m^2/s with a measured equilibrium t_{heal} value of 55 min.

Recent observations concerning room-temperature crack healing in epoxy thermosets using solvents at a crack interface[15] can be explained by similar mechanisms because a localized and temporary lowering of interfacial T_g below the ambient temperature in the presence of solvents could occur in such a system. It is interesting to note that free surfaces of cured epoxy–amine polymers do not exhibit healing when subjected to the same healing conditions, and this indicates that a fractured surface is necessary for interfacial adhesion to occur. It will be relevant to carry out experiments on surfaces with controlled roughness to further quantitatively assess effects on healing behavior.

Healing behavior at $r \neq 1$

Figure 6 is a plot of the fracture load of virgin specimens before and after the first heal ($T_{heal} = 185°C$, $t_{heal} = 1$ h) measured for specimens at different stoichiometric compositions. The data show that the average fracture load of virgin specimens increases with increasing amine content from 55 to 120 N for values of r from 1.4 to 0.82. The observed trend is consistent with work by Vanlandingham et al.[27] After the first healing cycle, this trend in the fracture strength with stoichiometry was not apparent. Figure 7 shows the corresponding healing efficiencies (i.e., ε_1) of these specimens at various values of r. For values of r between 0.82 and 1.07, ε_1 ranges between 50 and 70% without a distinct trend. These

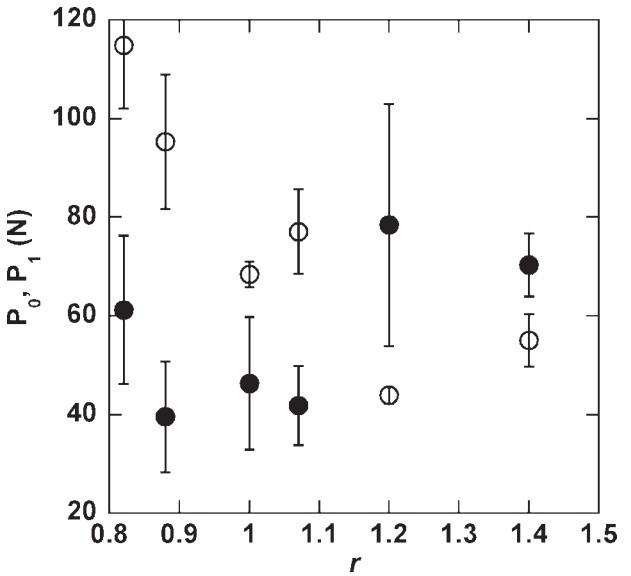

Figure 6 Plot of (○) the virgin fracture load (P_0) and (●) the fracture load after the first heal (P_1) versus r with healing under HP at $T_{heal} = 185°C$ and $t_{heal} = 1$ h.

results indicate that the bonding mechanism at the crack interface for these thermosets is not linked to specific differences of the polymer network structure arising from the stoichiometry employed but appears to be a more general phenomenon associated with epoxy–amine networks.

In the presence of a large excess of epoxide groups at $r = 1.2$ and $r = 1.4$, healing efficiencies of 178 ± 56 and 125 ± 10%, respectively, were observed; that is, the rehealed interface was stronger than that of virgin specimens. This is most likely due to interfacial reactions occurring during the healing cycle.

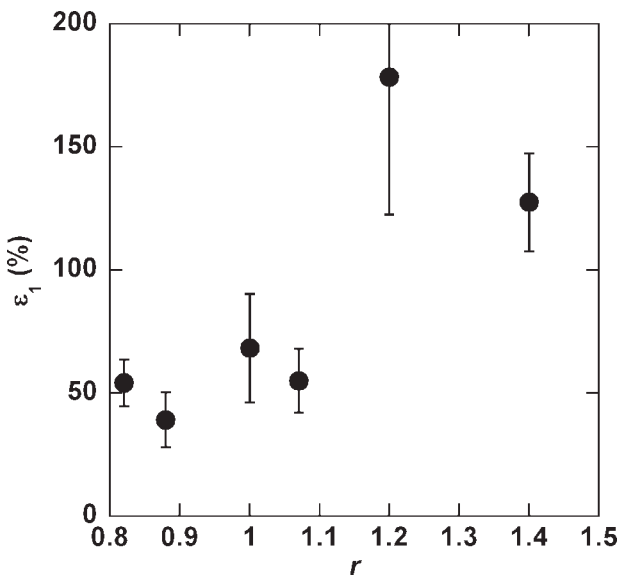

Figure 7 Plot of ε_1 versus r with healing under HP at $T_{heal} = 185°C$ and $t_{heal} = 1$ h.

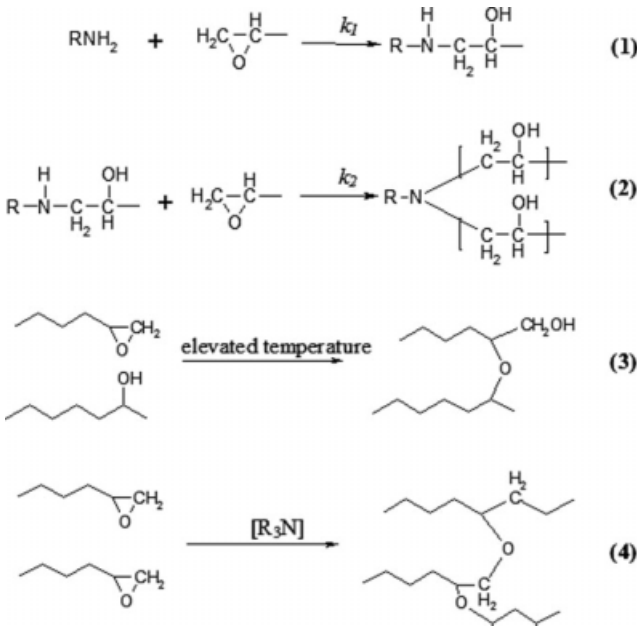

Figure 8 Chemical reactions for an epoxy–amine system: (1) epoxide ring opening with a primary amine followed by (2) epoxide ring opening with a secondary amine. Competing reactions may also take place via (3) etherification at elevated temperatures or (4) homopolymerization in the presence of tertiary amines.

Figure 8 shows the generalized reaction scheme between epoxy and amines (1 and 2), which results in the eventual formation of tertiary amine moieties.[1] Also included in Figure 8 are possible side reactions such as the high-temperature etherification reaction (3) and the related epoxy homopolymerization catalyzed by tertiary amines (4),[1] both of which can lead to differences in gel times and changes in the crosslink density depending on the cure temperature and time schedule. For the cycloaliphatic amine-cured DGEBA system, the side reactions are negligible during the cure cycle established to prepare samples. For specimens with $r > 1$ however, etherification and homopolymerization reactions (3 and 4) can occur, particularly at higher temperatures (T_{heal}) because unreacted epoxy groups are present.

Figure 9 shows plots of epoxy group consumption versus time obtained with near-infrared FTIR spectroscopy for an epoxy–amine thermoset with $r = 1.2$ at isothermal temperatures of 150, 185, and 200°C. After 3 h of exposure following curing, the concentration of the epoxy group decreased to 90% of the original concentration at 150°C, to 75% at 185°C, and to 55% at 200°C. The gradual decrease in the epoxy group concentration with time indicates that a slow reaction occurs. In a similar fashion, changes in unreacted amines were monitored for specimens with $r < 1$. The results did not indicate a change in the concentration to suggest the consumption of amines.

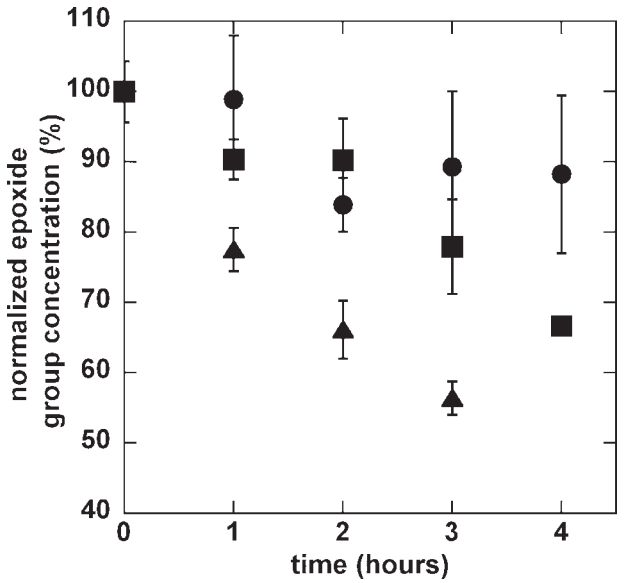

Figure 9 Consumption of epoxy groups (4528 cm^{-1}, near-infrared spectroscopy) at elevated temperatures plotted as the normalized concentration versus time at (●) 150, (■) 185, and (▲) 200°C.

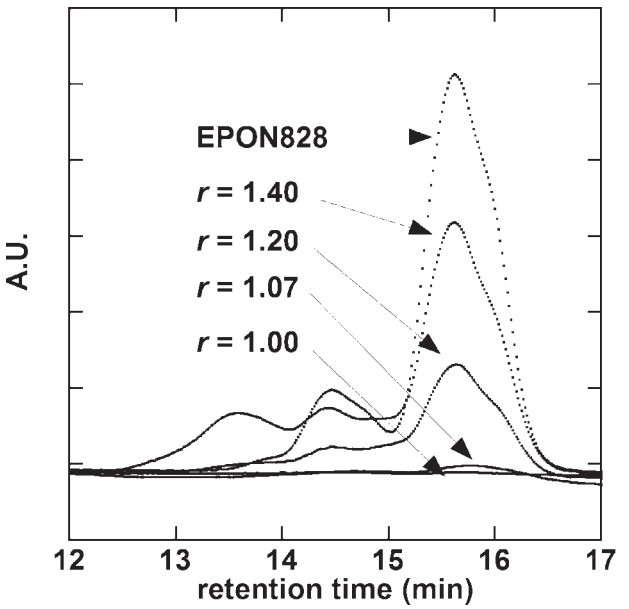

Figure 11 SEC traces of pure EPON-828 and extracts from epoxy–amine samples synthesized with r values of 1.40, 1.20, 1.07, and 1.00.

The occurrence and influence of these reactions were further evaluated through the monitoring of changes in T_g. Figure 10 is a plot of T_g evaluated for different stoichiometric ratios at different postcure temperatures. For specimens with $r = 1.4$, T_g increased from 80°C for the original cured sample to 116°C after a 3-h exposure at 185°C and to 118°C after an 8-h exposure at 200°C. This observed increase in T_g progressively decreased as r approached 1. For specimens with $r \leq 1$, exposure to high temperatures for prolonged periods of time (200°C for 8 h) did not significantly alter T_g. Therefore, the high strength gained during the first healing for specimens with an excess of epoxide groups was associated with etherification and homopolymerization reactions. This suggests that built-in secondary reaction mechanisms could be used effectively in the design of new self-healing systems.

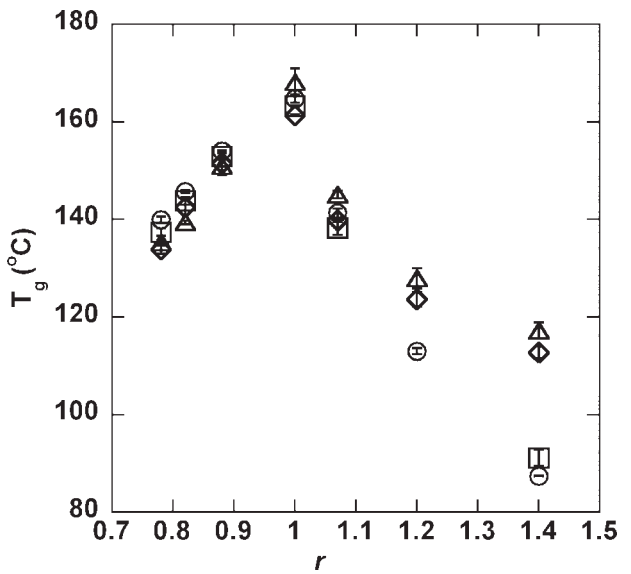

Figure 10 T_g of epoxy–amine samples with various stoichiometries evaluated from DSC measurements (○) after the original cure schedule and at (□) 1 h at 185°C, (◇) 3 h at 185°C, and (△) 8 h at 200°C beyond the original cure.

Off-stoichiometry reactions of epoxy–amine thermosets result not only in a lower crosslink density and reduced T_g but also in an incomplete reaction and an increased sol phase content. In the reaction of a diepoxy (difunctional) with a diamine (tetrafunctional), the sol phase content increases more significantly when excess epoxy rather than a paucity of epoxy is used. For the range of stoichiometries investigated, samples prepared at stoichiometry or with excess amine did not produce a measurable extractable sol phase. On the other hand, a significant sol phase was observed for samples synthesized with excess epoxy. Figure 11 shows SEC traces of extracts from epoxy–amine specimens with r ranging from 1.00 to 1.40 versus the SEC trace of EPON-828. This sol fraction showed a distribution of molecular weights up to a maximum of approximately 1000 g/mol according to polystyrene standards. The SEC traces also show the sol phase to be richer in DGEBA as r increases. This material was sufficiently mobile in the presence of THF to leach out of the polymer network, and its existence suggests that sol mobility may exist at elevated temperatures. Attempts were made to evaluate the weight fraction of the sol by Soxhlet extraction in THF followed by

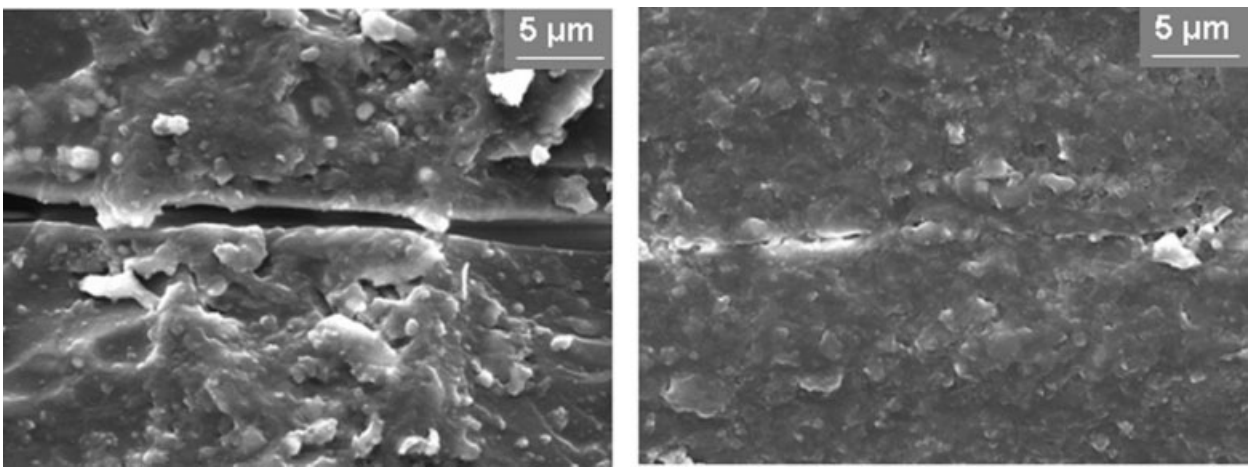

Figure 12 Scanning electron micrographs showing the crack interface at $r = 1.2$ after (left) the first fracture and (right) the first heal at $T_{heal} = 185°C$ and $t_{heal} = 10$ min under HP. Closure of the crack interface is indicated.

vacuum drying of all samples. Accurate trends to indicate weight losses were not possible because of significant dipole–dipole interactions between THF and the epoxy–amine network,[14] where complete removal of THF even at elevated temperatures was not possible.

Several models based on a statistical method or a combined kinetic–statistical method have been developed and used to predict a sol fraction within a thermosetting network.[33,34] Altering the reactant stoichiometric ratio alters the sol fraction, largely because of changes in the availability and chemical nature of the reactive sites. For systems cured off stoichiometry, differences in the sol fraction[33,35] are predicted on the basis of the molar excess, the chemical structure of the epoxy or amine used, and the cure schedule employed. Ideal networks tend to exhibit appreciable sol fractions beyond 60% excess amine concentrations or a 10% excess epoxy concentration. For systems such as ethylenediamine[35] and diamino diphenyl amine[36] cured epoxies, which exhibit significant substitution effects, sol formation is enhanced.[35] These predictions are supported by results obtained in this work, in which all excess epoxy concentrations had a measurable sol fraction, whereas for the range of excess amine concentrations investigated (up to 30%), a sol phase was not observed. This excess epoxy sol might contain unreacted species[37] or cyclic structures[38] depending on the reactivity or chemical structure of the monomer units. For DGEBA, it has been shown that cyclic structures are not formed[39] because of monomer rigidity and spatial separation between epoxide groups, and this suggests that the sol contains epoxide-bearing monomers and oligomers. For an epoxide-rich diffusible sol at $r > 1$ close to a crack interface, diffusion and reaction of this sol at the crack could result in a large concentration of covalent interfacial linkages and the large healing efficiencies discussed previously. These results suggest that enrichment of a crack interface with such mobile and reactive species may also enhance the crack-healing behavior of epoxy–amine thermosets.

Figure 12 shows micrographs of a specimen with $r = 1.2$ with a crack after the first fracture and a specimen with $r = 1.2$ with a healed crack (HP method, $T_{heal} = 185°C$, $t_{heal} = 10$ min). The fractured specimen clearly shows the presence of a crack with an average width of 1.5 μm between the crack interfaces. The micrograph for the healed specimen does not show such distinct separation between interfaces but rather indicates that with low t_{heal} values, adhesion has been achieved at multiple points along the interface, and a distinct crack is not visible even at high magnifications.

These reactions are expected to alter the time dependence of the healing efficiency. Figure 13 compares the healing efficiency at the first heal cycle for samples with $r = 1.2$ and $r = 0.82$ with the healing efficiency at $r = 1.0$ (discussed earlier in Fig. 4) for different t_{heal} values at $T_{heal} = 185°C$. For specimens with $r = 0.82$, the healing efficiency plateaus and never regains its original value even after 180 min. This suggests that interfacial contacts being formed never fully mimic the original network even after prolonged surface rearrangements; this is similar to observations for networks at $r = 1.0$. However, at $r = 1.2$, there is a strikingly higher increase in the healing efficiency with t_{heal} due to the previously discussed concurrent interfacial reactions. The specimens were found to recover their original fracture load within 30 min and reached an equilibrium value within 60 min. Figure 13 suggests a trend of a small but consistent drop in the healing efficiency for t_{heal} beyond 60 min, which might be due to a

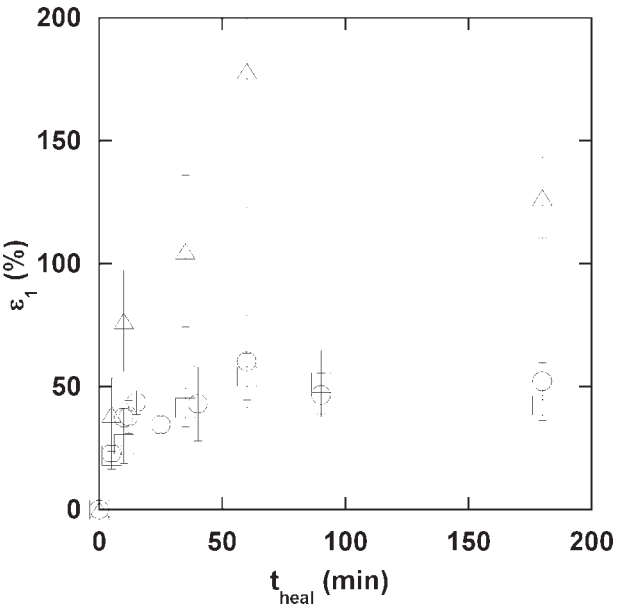

Figure 13 Plot of ε_1 versus t_{heal} determined at the first heal for specimens with (△) $r = 1.2$, (○) $r = 1$, and (□) $r = 0.82$. Samples were healed at $T_{heal} = 185°C$ under HP.

degradation of epoxy–amine specimens[40] after prolonged exposure to high temperatures. The data for $r = 1.2$ and $r = 0.82$ show a $t_{heal}1/2$ dependence similar to that observed for healing at $r = 1$.

The ability to heal multiple times observed for a stoichiometric epoxy–amine system was also observed off stoichiometry. Figure 14 presents a plot of ε_n' measured over four fracture and heal events for specimens with r between 0.82 and 1.2 ($T_{heal} = 185°C$ and $t_{heal} = 1$ h for each cycle). In all cases except for specimens with $r = 1.2$ on the first heal cycle, the recovered load was lower than the virgin fracture load and decreased with each cycle; this was similar to the case for specimens cured at stoichiometry (Fig. 3). Presumably at $r = 1.2$, the influence of the secondary reaction is curtailed after the first healing cycle by a depletion of free epoxies and/or the immobilization of the reactive sol phase. Nevertheless, all samples showed repeated healing upon cycling. The plot indicates that ε_n' plateaus to a value ranging between 60 and 80% for all stoichiometries and indicates a similar reduction in the ability to heal at every fracture cycle. It is possible that for the stoichiometries investigated, every fracture event results in a concomitant reduction of surface roughness, thereby reducing the interfacial surface area and the potential for mechanical interlocking described earlier. Thus, the cyclic fracture-healing process would tend to smooth the interface, provided that damage occurs along the same interface.

CONCLUSIONS

The results of this work suggest two distinct mechanisms responsible for healing in epoxy–amine thermosets synthesized at stoichiometry ($r = 1$) and off stoichiometry ($r \neq 1$). At stoichiometry, repeated crack healing was observed after multiple fracture and heal cycles for all specimens with and without any measurable reaction, extract phase, or changes in T_g. Healing was hypothesized in this case to be dominated by mechanical interlocking of nodular features on fracture surfaces. A 1/2 power dependence of strength recovery on t_{heal} was observed. Similar healing efficiencies were observed for specimens with $r < 1.07$, indicating that mechanical interlocking might be a common phenomenon in fractured epoxy–amine thermosets. Specimens with $r \gg 1$ showed a healing efficiency greater than 100%. This was attributed to a second mechanism of covalent bond formation due to polyetherification or homopolymerization reactions of unreacted epoxy groups at a crack interface. In addition, a measurable mobile sol fraction was observed for specimens with $r > 1$, suggesting enrichment of a crack interface with reactive epoxide groups. Such reactions increased the overall healing efficiency beyond that observed purely by mechanical interlocking. Specimens investigated at all stoichiometries exhibited the ability to heal repeatedly, although with a continuously decreasing value of the healing efficiency, which was suggested to be due to a gradual reduction of the interfacial surface area responsible for interlocking through attrition.

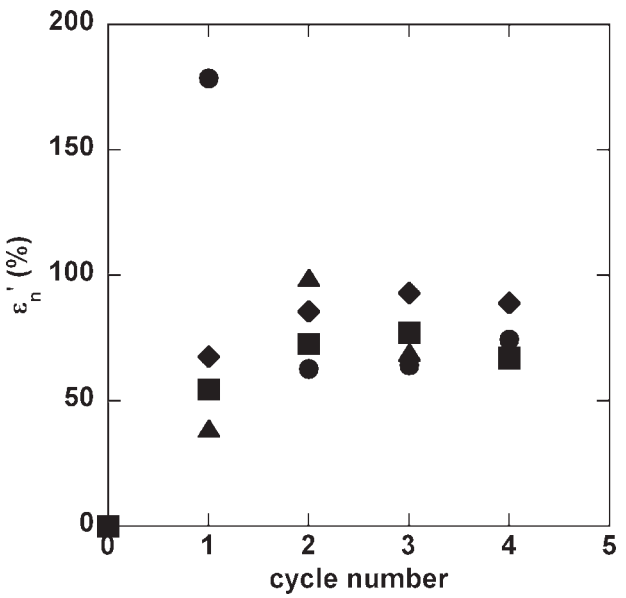

Figure 14 Plot of ε_n' for samples with (●) $r = 1.2$, (◆) $r = 1.0$, (▲) $r = 0.88$, and (■) $r = 0.82$ at $T_{heal} = 185°C$ and $t_{heal} = 1$ h at each cycle under HP.

References

1. Ellis, B. Chemistry and Technology of Epoxy Resins; Blackie Academic and Professional: Glasgow, 1993.
2. Pearson, R. A.; Yee, A. F. J Mater Sci 1991, 26, 3828.
3. Pearson, R. A.; Yee, A. F. Polymer 1993, 34, 3658.
4. Dry, C. M. Proc SPIE; 1994; Vol. 2189, p 62.
5. White, S. R.; Sottos, N. R.; Geubelle, P. H.; Moore, J. S.; Kessler, M. R.; Sriram, S. R.; Brown, E. N.; Viswanathan, S. Nature 2001, 409, 794.
6. Williams, G.; Trask, R.; Bond, I. Compos A 2007, 38, 1525.
7. Chen, X.; Dam, M. A.; Ono, K.; Mal, A.; Shen, H.; Nutt, S. R.; Sheran, K.; Wudl, F. Science 2002, 295, 1698.
8. Chen, X.; Wudl, F.; Mal, A. K.; Shen, H.; Nutt, S. R. Macromolecules 2003, 36, 1802.
9. Hayes, S. A.; Jones, F. R.; Marshiya, K.; Zhang, W. Compos A 2007, 38, 1116.
10. Outwater, J. O.; Gerry, D. J. J Adhes 1969, 1, 290.
11. Wool, R. P. Polymer Interfaces: Structure and Strength; Hanser-Gardener: New York, 1995.
12. Lee, H.; Neville, K. Handbook of Epoxy Resins; McGraw-Hill: New York, 1967.
13. Rahmathullah, A. M.; Palmese, G. R. Proceedings of the 1st International Conference on Self-Healing Materials; in Self-Healing Materials: An Alternative Approach to 20 Centuries of Materials Science; Springer Series in Materials Science; VanderZwaag, S., Eds.; April 18–20, Noordwijk aan Zee, The Netherlands, 2007, Vol. 100.
14. Raman, V. I.; Palmese, G. R. Macromolecules 2005, 38, 6923.
15. Caruso, M. M.; Delafuente, D. A.; Ho, V.; Sottos, N. R.; Moore, J. S.; White, S. R. Macromolecules 2007, 40, 8830.
16. Palmese, G. R.; McCullough, R. L. J Appl Polym Sci 1992, 46, 1863.
17. Fu, J. H.; Schlup, J. R. J Appl Polym Sci 1993, 49, 219.
18. Singh, K. P.; Palmese, G. R. J Appl Polym Sci 2004, 91, 3107.
19. Raghavan, J.; Wool, R. P. J Appl Polym Sci 1999, 71, 775.
20. van Krevelen, D. W. Properties of Polymers: Their Correlation with Chemical Structure; Their Numerical Estimation and Prediction from Additive Group Contributions; Elsevier: Amsterdam, 1990.
21. Kim, Y. H.; Wool, R. P. Macromolecules 1983, 16, 1115.
22. Prager, S.; Adolf, D.; Tirrell, M. J Chem Phys 1986, 84, 5152.
23. Gennes, P. G. D. J Chem Phys 1971, 55, 572.
24. Wool, R. P.; O'Connor, K. M. J Appl Phys 1981, 52, 5953.
25. Yamaguchi, M.; Ono, S.; Terano, M. Mater Lett 2007, 61, 1396.
26. Antonietti, M.; Sillescu, H. Macromolecules 1985, 18, 1162.
27. Vanlandingham, M. R.; Eduljee, R. F.; Gillespie, J. W., Jr. J Appl Polym Sci 1999, 71, 699.
28. Duchet, J.; Pascault, J. P. J Polym Sci Part B: Polym Phys 2003, 41, 2422.
29. Kishi, H.; Naitou, T.; Matsuda, S.; Murakami, A.; Muraji, Y.; Nakagawa, Y. J Polym Sci Part B: Polym Phys 2007, 45, 1425.
30. Wetzel, B.; Haupert, F.; Qiu Zhang, M. Compos Sci Technol 2003, 63, 2055.
31. Deen, W. M. Analysis of Transport Phenomena; Oxford University Press: New York, 1998.
32. Jud, K.; Kausch, H. H. Polym Bull 1979, 1, 697.
33. Riccardi, C. C.; Williams, R. J. J. Polymer 1986, 27, 913.
34. Miller, D. R.; Macosko, C. W. Macromolecules 1976, 9, 206.
35. Vallo, C. I.; Frontini, P. M.; Williams, R. J. J. J Polym Sci Part B: Polym Phys 1991, 29, 1503.
36. Charlesworth, J. M. J Polym Sci Polym Phys Ed 1979, 17, 1557.
37. Riccardi, C. C.; Williams, R. J. J. J Appl Polym Sci 1986, 32, 3445.
38. Matejka, L.; Dusek, K. Macromolecules 1989, 22, 2902.
39. Matejka, L.; Podzimek, S.; Dusek, K. J Polym Sci Part A: Polym Chem 1995, 33, 480.
40. Dyakonov, T.; Mann, P. J.; Yan, C.; Stevenson, W. T. K. Polym Degrad Stab 1996, 54, 67.